Parameter-varying Modelling and Fault Reconstruction for Wind Turbine Systems

Hui Shao[1], Zhiwei Gao[2], Xiaoxu Liu[2] and Krishna Busawon[2]

[1]College of Information Science and Engineering, Huaqiao University, China

[2]Faculty of Engineering and Environment, University of Northumbria, UK

*Author to whom correspondence should be addressed; Email: shaohuihu11@hotmail.com; zhiwei.gao@northumbria.ac.uk; Tel.:+86-180-30076128; +44-776-5977948

Abstract: In this paper, parameter-varying technique is firstly addressed for modelling a 4.8MW wind turbine system which is nonlinear in essence. It is worthy to point out that the proposed parameter-varying model is capable of describing a nonlinear real-time process by using real-time system parameter updating. Secondly, fault reconstruction approach is proposed to reconstruct system component fault and actuator fault by utilizing augmented adaptive observer technique with parameter-varying. Different from the offline tuning adaptive scheme, the proposed adaptive observer includes adaptive tuning ability to online adjust the observer based on varying parameter. The effectiveness of the proposed parameter-varying modelling and fault reconstruction methods is demonstrated by using a widely-recognized 4.8 MW wind turbine benchmark system.

Keywords: Adaptive observer; Fault diagnosis; Fault reconstruction; Parameter-varying modeling; Wind turbine systems;

1. Introduction

Recently, wind turbine industries have been rapidly developed which have dominated renewable energy market. Since most of the wind power systems are placed along mountains, farmland, coastline, and even in seas, it is challenging to maintain and repair them timely when any unexpected faults occur in the wind turbine system. Therefore there is a high demand to improve the system reliability of the wind turbine systems by implementing effective real-time monitoring and fault diagnosis [1, 2]. Fault diagnosis methods can be generally categorized into model-based approach, signal-based approach and data-driven approach [3-6]. Model-based fault diagnosis is one of the most powerful and popular system monitoring and fault diagnosis methods for wind turbine systems, and some results were reported in [7-13], generally utilizing linearized time-invariant models of wind turbine systems. However, wind turbines are nonlinear or parameter time-varying in nature. Therefore, linear time-invariant models at some operation points would fail to describe the global wind turbine system performance. In particular, nonlinearities in the aerodynamic torque are indispensable [14, 15]. In order to better describe wind turbine systems, parameter-varying models or fuzzy models were utilized for modelling wind turbine systems [16-19]. Based on linear parameter-varying models, a variety of approaches for control synthesis, monitoring and fault diagnosis for wind turbine systems were also addressed in [20-25]. However, a big concern is the complexity of the design and implementation by using the aforementioned methods in [20-25]. In addition, it could cause system oscillation when control or observation switching strategies were used. Therefore, there is a strong motivation to develop a novel modelling and real-time monitoring techniques for wind turbine systems. In this paper, a novel parameter-varying model for wind turbine systems is established, which is used for real-time monitoring and fault reconstruction in wind turbine systems.

Adaptive observation and regulation play an important role in system analysis and control synthesis, and some interesting results are reported on the basis of time-varying parameter models. In [26], an

adaptive control method with exponential regulation in a parameter-varying model was addressed. In [27], time-varying parameter adaptive control was investigated. A periodic parameter adaptation approach for time-varying parametric uncertain systems was discussed in [28]. It is noticed that most of the approaches in [26-28] are Lyapunov function based methods, where it is a challenging to find a proper Lyapunov function for the system stability analysis, as well as not easy to solve and implement for some cases, for instance, the case for system with varying parameters at arbitrary velocity [28].

In this paper, a novel observer is constructed with adaptive parameters tuning for fault reconstruction based on the proposed parameter-varying model. It is designed offline, but performed and regulated automatically on-line for real-time monitoring and fault diagnosis. The augmented system approach and the parameter-varying model are integrated for designing this novel fault estimator to simultaneously reconstruct the concerned faults as well as system states. From the error dynamics analysis and simulation results, it can be concluded that the proposed adaptive parameter-varying observer possesses a certain ability of disturbance rejection, apart from being able to estimate system states and reconstruct system faults.

The paper is organized as follows. Parameter-varying modeling for wind turbine is discussed in Section **2**. Faulty system for wind turbine systems with concerned component fault and actuator fault is addressed in Section **3**. Parameter-varying-model based states observation and fault reconstruction for wind turbine systems is investigated in Section **4**. Validation studies on a 4.8 MW wind turbine benchmark are addressed in Section **5**. The paper is ended with conclusion in Section **6**.

2. Parameter-varying Modeling for Wind Turbine

Due to highly nonlinearity and random uncontrolled driving wind, wind turbines should be identified along the global operating region. Parameter-varying modelling is an effective method to build a model to describe the wind turbine operation. However, conventional parameter-varying models generally possess nonlinear switched affine structures, which may bring complexity and challenges in the design and

implementation of the model-based controller and fault detector. In order to overcome the potential drawbacks of the conventional parameter-varying modelling methods, a novel parameter-varying model for wind turbine system is built by using real-time parameter updating.

A 4.8MW benchmark wind turbine system [25] is depicted by Figure 1, which is composed of aerodynamics and blade system, drive train and generator, and the symbols in Figure 1 are listed in Table 1.

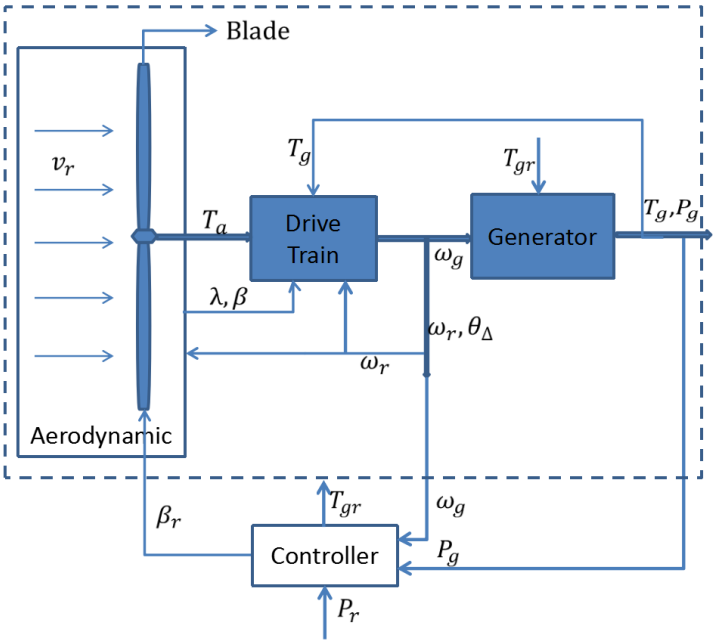

Figure 1. Wind turbine's architecture

Table 1. System parameters I

Symbols	Quantity	Unit
v_r	Wind speed	m/s
T_a	Aerodynamic torque	Nm
λ	Tip-speed-ratio	[·]
β	Blade pitch angle	°
β_r	Reference blade pitch angle	°
ω_r	Rotor speed	Rad/s
T_{gr}	Reference generator torque	Nm
ω_g	Generator speed	Rad/s
T_g	Generator torque	Nm
P_g	Generator power	MW
P_r	Reference generator power	MW
θ_Δ	Torsion angle of the drive train	°

79

80 *2.1. Aerodynamic Model*

81 The aerodynamic torque T_a acting on the blades is:

82 $$T_a = \frac{p_m}{\omega_r} = \frac{1}{2}\rho\pi R^3 C_q(\lambda,\beta)v_r^2 \quad (1)$$

83 where P_m denotes the mechanical power, ρ is the air density [Kg/m^3], R is the radius of the rotor [m],
84 and v_r is the wind speed limited to 0~25[m/s], $C_q(\lambda,\beta)$ is the torque coefficient which is a strong non-
85 linear term, depending on the blade pitch angle β, and the tip-speed-ratio λ defined as $\lambda = \omega_r R/v_r$.
86 The relationship between $C_q(\lambda,\beta)$ and λ,β is generally characterized by a Lookup Table scheme,
87 which cannot be utilized directly in model-based control and observation design and implementation.

88 From Eq.(1), one can see the nonlinearity of the torque T_a is caused by v_r^2 and $C_q(\lambda,\beta)$. In this study,
89 we construct a nonlinear polynomial function to illustrate the nonlinear dynamics. Here, $C_q(\lambda,\beta)$ will be
90 identified by the curve fitting method using the real data and Linear Least Square method, which is
91 carried out by using Matlab Curve Fitting Toolbox, described as follows by using the polynomial of the
92 two input parameters:

93 $$C_q(\lambda,\beta) = p_{00} + p_{10}\lambda + p_{01}\beta + p_{11}\lambda\beta + p_{20}\lambda^2 + p_{02}\beta^2 + \cdots + p_{k0}\lambda^k + p_{0l}\beta^l \quad (2)$$

94 where $p_{00}, p_{10}, p_{01}\cdots p_{0l}$ are the coefficients of the polynomial, k and l are the orders of the polynomial
95 illustrating the curve fitting accuracy. By replacing the Lookup Table, the obtained polynomial equation
96 of C_q can be used on line.

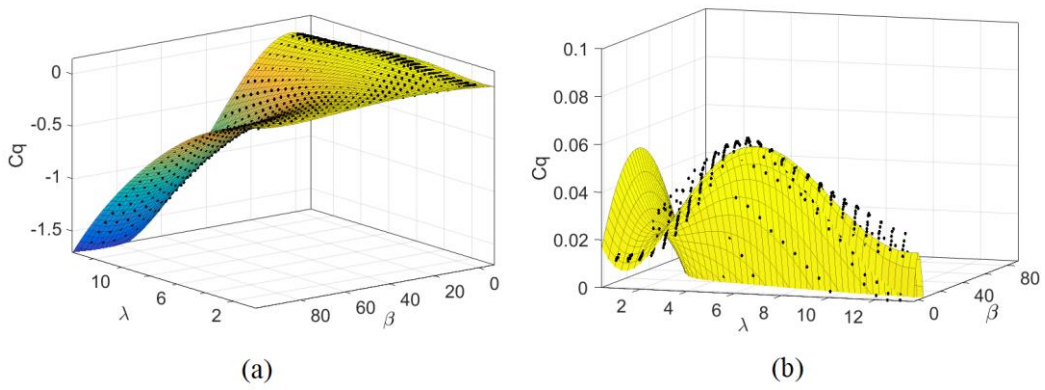

Figure 2. (a) Real data (Dot) and fitting curve result (Color surface) of torque coefficient C_q;

(b) Zoom-in curve of C_q.

Figure 2 depicts the curve $C_q(\lambda,\beta)$ against the pitch angle β and tip-speed-ratio λ. In Figure 2a, the black dot shows the real data of the measurement used as the Lookup Table in [25], and the color surface shows the curve fitting result of $C_q(\lambda,\beta)$. It is noticed that $C_q(\lambda,\beta)$ can take values either positive or negative, which correspond to the generation mode or motor mode, respectively [29]. From the zoom-in Figure 2b, one can see $C_q(\lambda,\beta)$ takes positive values when the generator works in generation mode.

Substituting $v_r = \omega_r R/\lambda$ to Eq.(1), T_a is rewritten as:

$$T_a = \frac{p_m}{\omega_r} = \frac{1}{2}\rho\pi R^5 C_q(\lambda,\beta)\,\omega_r^2/\lambda^2 \tag{3}$$

Obviously, the nonlinearity of the torque T_a is caused by ω_r/λ and $C_q(\lambda,\beta)$.

For the above mentioned β, the state-space representation is given as follows [25]:

$$\begin{bmatrix}\dot{\beta}(t)\\ \ddot{\beta}_0(t)\end{bmatrix} = \begin{bmatrix}0 & \omega_n^2\\ -1 & -2\varsigma\omega_n^2\end{bmatrix}\begin{bmatrix}\beta(t)\\ \dot{\beta}_0(t)\end{bmatrix} + \begin{bmatrix}0\\ 1\end{bmatrix}\beta_r(t) \tag{4}$$

where ω_n and ς denote the natural frequency and damping ratio respectively; β and β_r are respectively the pitch angle and its reference value with the changing range [-2°~95°], and $\beta_0 = \frac{1}{\omega_n^2}\dot{\beta}$ is proportional to the change rate of the pitch angle.

2.2. Drive Train and Generator Model

From [25], we can see the drive train dynamics including gear box is subjected to the most of prominent nonlinear dynamics of a wind turbine system. The two-mass drive train model is driven by the two inputs: the aero dynamic torque T_a and the generator torque T_g, which make the nonlinear dynamics distributed in the state matrix and input matrix separately in the state-space equation. In this paper, the system is expressed as a parameter-varying model with only one input from the generator torque T_g as follows:

$$\begin{pmatrix} \dot{\omega}_r(t) \\ \dot{\omega}_g(t) \\ \dot{\theta}_\Delta(t) \end{pmatrix} = \begin{pmatrix} a_{11}(\lambda,\beta,\omega_r) & \frac{B_{dt}}{n_g J_r} & -\frac{K_{dt}}{J_r} \\ \frac{\eta_{dt}B_{dt}}{n_g J_g} & a_{22} & \frac{\eta_{dt}K_{dt}}{n_g J_g} \\ 1 & -\frac{1}{n_g} & 0 \end{pmatrix} \begin{pmatrix} \omega_r(t) \\ \omega_g(t) \\ \theta_\Delta(t) \end{pmatrix} + \begin{pmatrix} 0 \\ -\frac{1}{J_g} \\ 0 \end{pmatrix} T_g(t) \tag{5}$$

where

$$a_{11}(\lambda,\beta,\omega_r) = -\frac{B_{dt}+B_r}{J_r} + \frac{T_a^{'}}{J_r},\ a_{22} = -\frac{\eta_{dt}B_{dt}}{n_g^2 J_g} - \frac{B_g}{J_g},\ T_a^{'} = \frac{T_a}{\omega_r} = \frac{1}{2}\rho\pi R^5 C_q(\lambda,\beta)\omega_r/\lambda^2$$

and *k* and *l* in Eq.(2) both equal to 5, namely, $C_q(\lambda,\beta) = p_{00} + p_{10}\lambda + p_{01}\beta \cdots + p_{50}\lambda^5 + p_{05}\beta^5$. From the above, it is indicated that $a_{11}(\lambda,\beta,\omega_r)$ is a nonlinear function of β,λ and ω_r. For simplicity, $a_{11}(\lambda,\beta,\omega_r)$ is denoted as a_{11} in the rest of the paper.

The generator and converter dynamics can be modelled as a first-order dynamics:

(6)

where τ_g is the time constant of the model. The power produced by the generator is given by $P_g(t) = \eta_g \omega_g(t) T_g(t)$, where η_g is the efficiency of the generator.

The parameters of the system are shown in Table 2 [25].

Table 2. System parameters II

Symbols	Quantity	Parameter	Unit
J_r	Moment of inertia of the low-speed shaft	55×10^6	kgm^2
B_{dt}	Drive train's torsion damping coefficient	775.49	Nms/rad
n_g	Gear ratio	95	[·]
K_{dt}	Torsion stiffness of the drive train	2.7×10^9	Nms/rad
J_g	Moment of inertia of the high-speed shaft	390	kgm^2
B_r	Rotor external damping	7.11	Nms/rad
B_g	Viscous friction of the high-speed shaft	45.6	Nms/rad
η_{dt}	Efficiency of the drive train	0.97	[·]
ω_n	Natural frequency	11.11	Rad/s
ς	Damping ration	0.6	[·]
τ_g	Time constant	0.02	s/rad

2.3. Parameter-varying Model of Wind Turbine

On the basis of the subsections *2.1* and *2.2*, the parameter-varying model of overall wind turbine system can be derived as follows:

$$\begin{cases} \dot{x}(t) = A(\lambda, \beta, \omega_r)x(t) + Bu(t) \\ y(t) = Cx(t) \end{cases} \tag{7}$$

where

$$x(t) = \begin{bmatrix} \omega_r(t) & \omega_g(t) & \theta_\Delta(t) & \beta(t) & \dot{\beta}_0(t) & T_g(t) \end{bmatrix}^T,\ u(t) = \begin{bmatrix} T_{gr}(t) & \beta_r(t) \end{bmatrix}^T,$$

$$y(t) = \begin{bmatrix} \omega_r(t) & \beta(t) & T_g(t) & \omega_g(t) \end{bmatrix}.$$

β, λ and ω_r are the scheduling parameters, β and ω_r can be measured to real-time update the model, λ can be calculated by the measuring variables v_r and ω_r. $A_{11}(\lambda, \beta, \omega_r)$, *B*, *C* are shown as follows:

148
$$A(\lambda,\beta,\omega_r)=\begin{pmatrix} a_{11}(\lambda,\beta,\omega_r) & \frac{B_{dt}}{n_g J_r} & -\frac{K_{dt}}{J_r} & 0 & 0 & 0 \\ \frac{\eta_{dt}B_{dt}}{n_g J_g} & a_{22} & \frac{\eta_{dt}K_{dt}}{n_g J_g} & 0 & 0 & -\frac{1}{J_g} \\ 1 & -\frac{1}{n_g} & 0 & 0 & 0 & 0 \\ 0 & 0 & 0 & 0 & \omega_n^2 & 0 \\ 0 & 0 & 0 & -1 & -2\zeta\omega_n & 0 \\ 0 & 0 & 0 & 0 & 0 & -\frac{1}{\tau_g} \end{pmatrix}, \quad B=\begin{pmatrix} 0 & 0 \\ 0 & 0 \\ 0 & 0 \\ 0 & 0 \\ 0 & 1 \\ \frac{1}{\tau_g} & 0 \end{pmatrix}, \quad C=\begin{pmatrix} 1 & 0 & 0 & 0 & 0 & 0 \\ 0 & 0 & 0 & 1 & 0 & 0 \\ 0 & 0 & 0 & 0 & 0 & 1 \\ 0 & 1 & 0 & 0 & 0 & 0 \end{pmatrix}. \quad (8)$$

149 ## 3. Wind Turbine System Subjected to Faults

150 By taking into account the component fault and actuator fault, the parameter-varying wind turbine model
151 can be represented by:

152
$$\begin{cases} \dot{x}(t) = A(\lambda,\beta,\omega_r)x(t) + Bu(t) + B_a f_{au}(t) \\ \qquad\quad + B_c f_c(t) + B_d d(t) \\ y(t) = Cx(t) \end{cases} \quad (9)$$

153 where $x(t) \in R^n$ represents the state vector, $u(t) \in R^m$ is input vector, $f_{au}(t) \in R^{k_a}$ is actuator fault vector,
154 $f_c(t) \in R^{k_c}$ is the component fault vector, $d(t) \in R^{k_d}$ stands for the process disturbance vector, $y(t) \in R^p$ is the
155 measurement output vector; B_a , B_c and B_d are the distribution matrices of the actuator faults, component faults and
156 process disturbances. For the wind turbine system, $n = 6$, $p = 4$ and $m = 2$, and $A_{11}(\lambda,\beta,\omega_r)$, B, C are defined
157 as in (8).

158 In order to reconstruct the faults concerned, we construct an augmented system as follows:

159
$$\begin{cases} \dot{x}_e(t) = A_e(\lambda,\beta,\omega_r)x_e(t) + B_e u(t) + B_{de} d_e(t) \\ y(t) = C_e x(t) \end{cases} \quad (10)$$

160 where $x_e(t)=\begin{pmatrix} x(t) \\ f(t) \end{pmatrix}$, $A_e(\lambda,\beta,\omega_r)=\begin{pmatrix} A(\lambda,\beta,\omega_r) & B_{ac} \\ \mathbf{0}_{k\times n} & \mathbf{0}_{k\times k} \end{pmatrix}$, $B_{ac}=\begin{pmatrix} B_a & B_c \end{pmatrix}$, $B_e=\begin{pmatrix} B \\ \mathbf{0}_{k\times m} \end{pmatrix}$, $B_{de}=\begin{pmatrix} B_d & 0 \\ 0 & I_k \end{pmatrix}$,

161

$C_e = \begin{pmatrix} C & \mathbf{0}_{p\times k} \end{pmatrix}$, k is the total number of the concerned faults, $d_e(t) = \begin{pmatrix} d(t) \\ \dot{f}(t) \end{pmatrix}$, and $f = \begin{pmatrix} f_{au} \\ f_c \end{pmatrix}$ represents the faults to be reconstructed. Here, the faults are assumed to be slow-varying, which can cover the typical faults in engineering systems such as abrupt faults and incipient faults by assuming $\dot{f}(t)$ to be bounded.

In this paper, the parameter fault and the actuator fault are both considered. The parameter B_g is assumed to have an additive fault, denoted by B_{gf}. As a result, the resulting fault and distribution matrix can be respectively represented by

$$f_c = -\frac{B_{gf}\omega_g}{J_g}, \text{ and } B_c = \begin{pmatrix} 0 & 1 & 0 & 0 & 0 & 0 \end{pmatrix}^T$$

The generator torque is assumed to be faulty, and its distribution matrix is expressed as:

$$B_a = \begin{pmatrix} 0 & 0 & 0 & 0 & 0 & \frac{1}{\tau_g} \end{pmatrix}^T$$

In order to simplify formulas, $A_e(\lambda, \beta, \omega_r)$ is abbreviated as A_e in the following sections.

4. Parameter-varying model-based observer

4.1. Design of Parameter-varying Model-based Observer

As there are only four independent columns in the output system matrix C_e, we can make the first four columns of the C_e are independent, but the others are zero by using some coordination transformations. In other words, we can make a simple change of the coordinates so that all the non-zero elements in the system output matrix will appear in the first four columns only. More precisely, we set:

$$z(t) = Px_e(t) \tag{11}$$

where

$$z=\begin{pmatrix} z_1 \\ z_2 \\ z_3 \\ z_4 \\ z_5 \\ z_6 \\ z_7 \\ z_8 \end{pmatrix}, x_e=\begin{pmatrix} x_1 \\ x_2 \\ x_4 \\ x_6 \\ x_3 \\ x_5 \\ x_7 \\ x_8 \end{pmatrix}, P=\begin{pmatrix} 1 & 0 & 0 & 0 & 0 & 0 & 0 & 0 \\ 0 & 1 & 0 & 0 & 0 & 0 & 0 & 0 \\ 0 & 0 & 0 & 1 & 0 & 0 & 0 & 0 \\ 0 & 0 & 0 & 0 & 0 & 1 & 0 & 0 \\ 0 & 0 & 1 & 0 & 0 & 0 & 0 & 0 \\ 0 & 0 & 0 & 0 & 1 & 0 & 0 & 0 \\ 0 & 0 & 0 & 0 & 0 & 0 & 1 & 0 \\ 0 & 0 & 0 & 0 & 0 & 0 & 0 & 1 \end{pmatrix}$$

As two faults are considered, the dimension of the augmented system state is $n+k=8$. Via the coordination transformation (11), the augmented system (10) becomes:

$$\begin{cases} \dot{z}(t)=Fz(t)+Gu(t)+Jd_e(t) \\ y(t)=Hz(t) \end{cases} \tag{12}$$

where $F=PA_eP^{-1}$, $G=PB_e$, $H=C_eP^{-1}$, $J=PB_{de}$.

The observability matrix is given by:

$$\overline{O}=\begin{pmatrix} H \\ HF \\ HF^{2} \\ \vdots \\ HF^{(n+k-1)} \end{pmatrix}=\begin{pmatrix} O \\ HF^{2} \\ \vdots \\ HF^{(n+k-1)} \end{pmatrix}=\begin{pmatrix} 1 & 0 & 0 & 0 & 0 & 0 & 0 & 0 \\ 0 & 1 & 0 & 0 & 0 & 0 & 0 & 0 \\ 0 & 0 & 1 & 0 & 0 & 0 & 0 & 0 \\ 0 & 0 & 0 & 1 & 0 & 0 & 0 & 0 \\ a_{11} & \frac{1}{J_r n_g}B_{dt} & 0 & 0 & 0 & -\frac{1}{J_r}K_{dt} & 0 & 0 \\ \frac{\eta_{dt}B_{dt}}{J_g n_g} & a_{22} & 0 & -\frac{1}{J_g} & 0 & \frac{\eta_{dt}K_{dt}}{J_g n_g} & 0 & 1 \\ 0 & 0 & 0 & 0 & \omega_0^2 & 0 & 0 & 0 \\ 0 & 0 & 0 & -\frac{1}{\tau_g} & 0 & 0 & \frac{1}{\tau_g} & 0 \\ & & & \cdots & & & & \end{pmatrix} \tag{13}$$

From (13), one can find that $\operatorname{rank}\overline{O}=n+k=8$, which indicates the system (12) is observable. As a result, one can make another linear transformation in order to transform the system into an observable canonical form.

Let

$$\xi(t)=Oz(t) \tag{14}$$

one can have

193
$$\begin{cases} \dot{\xi}(t) = O\dot{z}(t) = OFO^{-1}\xi(t) + OGu(t) + OJd_e(t) \\ \quad = \overline{A}_e\xi(t) + \overline{B}_e u(t) + \overline{B}_{de} d_e(t) \\ y(t) = Hz(t) = HO^{-1}\xi(t) = H_e\xi(t) \end{cases} \tag{15}$$

194 where

195
$$\overline{A}_e = \begin{pmatrix} \mathbf{0}_{4\times4} & I_4 \\ \overline{A}_{21} & \overline{A}_{22} \end{pmatrix},\ \overline{B}_e = \begin{pmatrix} \overline{B}_1 \\ \overline{B}_2 \end{pmatrix},$$
$$\overline{B}_{de} = \begin{pmatrix} \overline{B}_{d1} \\ \overline{B}_{d2} \end{pmatrix}, H = H_e = \begin{pmatrix} I_4 & \mathbf{0}_{4\times4} \end{pmatrix}$$

196
$$\overline{A}_{21} = \begin{pmatrix} -\frac{K_{dt}}{J_r} - \frac{B_{dt}}{J_g J_r n_g^2} & \frac{K_{dt}}{J_r n_g} & 0 & 0 \\ \frac{K_{dt}\eta_{dt}}{J_g n_g} & -\frac{K_{dt}\eta_{dt}}{J_g n_g^2} & 0 & 0 \\ 0 & 0 & -\omega^4 & 0 \\ 0 & 0 & 0 & 0 \end{pmatrix}, \overline{A}_{22} = \begin{pmatrix} a_{11} & \frac{B_{dt}}{J_r n_g} & 0 & 0 \\ \frac{B_{dt}\eta_{dt}}{J_g n_g} & a_{22} & 0 & -\frac{1}{J_g} \\ 0 & 0 & -2\zeta_0\omega_0 & 0 \\ 0 & 0 & 0 & -\frac{1}{\tau_g} \end{pmatrix},$$

197
$$\overline{B}_1 = \begin{pmatrix} 0 & 0 \\ 0 & 0 \\ \frac{1}{\tau_g} & 0 \\ 0 & 0 \end{pmatrix}, \overline{B}_2 = \begin{pmatrix} 0 & a_{11} \\ -\frac{1}{J_g\tau_g} & \frac{B_{dt}\eta_{dt}}{J_g n_g} \\ 0 & 0 \\ -\frac{1}{\tau_g^2} & 0 \end{pmatrix}.$$

198 An observer for this transformed system can be designed as follows:

199
$$\dot{\hat{\xi}}(t) = \overline{A}_e\hat{\xi}(t) + \overline{B}_e u(t) + L(y(t) - H_e\hat{\xi}(t)) \tag{16}$$

200 where $L = \begin{pmatrix} \mathbf{0}_{4\times4} \\ \overline{A}_{21} \end{pmatrix} + \begin{pmatrix} 2\theta I_4 \\ \theta^2 I_4 \end{pmatrix}$, $\theta > 0$. It is notice that the observer gain can be real-time updated as the

201 parameters $\overline{A}_{21}$ is real-time updating. Therefore, the observer (16) can be called adaptive observer as it

202 can update gain adaptively when the system parameters are changing.

203 Letting $\varepsilon(t) = \xi(t) - \hat{\xi}(t)$, the error dynamic of the observer is given by:

$$
\begin{aligned}
\dot{\varepsilon}(t) &= \left(\overline{A}_e - LH_e\right)\varepsilon(t) + \overline{B}_{de} d_e(t) \\
&= \left[\begin{pmatrix} \mathbf{0}_{4\times4} & I_4 \\ \overline{A}_{21} & \overline{A}_{22} \end{pmatrix} - \begin{pmatrix} 2\theta I_4 & \mathbf{0}_{4\times4} \\ \overline{A}_{21} + \theta^2 I_4 & \mathbf{0}_{4\times4} \end{pmatrix}\right]\varepsilon(t) + \overline{B}_{de} d_e(t) \\
&= \begin{pmatrix} -2\theta I_4 & I_4 \\ -\theta^2 I_4 & \overline{A}_{22} \end{pmatrix}\varepsilon + \overline{B}_{de} d_e(t)
\end{aligned} \tag{17}
$$

Let $\varepsilon(t) = \left(\varepsilon_1(t) \quad \varepsilon_2(t)\right)^T$, the error dynamic (17) is rewritten as:

$$
\begin{aligned}
\dot{\varepsilon}(t) &= \begin{pmatrix} -2\theta I_4 & I_4 \\ -\theta^2 I_4 & \mathbf{0}_{4\times4} \end{pmatrix}\varepsilon(t) + \overline{B}_{de} d_e(t) + \begin{pmatrix} 0 \\ \overline{A}_{22}\varepsilon_2(t) \end{pmatrix} \\
&= A_\varepsilon \varepsilon(t) + \overline{B}_{de} d_e(t) + \Delta\varepsilon(t)
\end{aligned} \tag{18}
$$

Consider the linear transformation:

$$
\bar{\varepsilon}(t) = \begin{pmatrix} I_4/\theta & \mathbf{0}_{4\times4} \\ \mathbf{0}_{4\times4} & I_4/\theta^2 \end{pmatrix}\varepsilon(t) = P_\varepsilon \varepsilon(t)
$$

one has

$$
\begin{aligned}
\dot{\bar{\varepsilon}}(t) &= P_\varepsilon \dot{\varepsilon}(t) = P_\varepsilon A_\varepsilon P_\varepsilon^{-1}\bar{\varepsilon}(t) + P_\varepsilon \Delta\varepsilon(t) + P_\varepsilon \overline{B}_{de} d_e(t) \\
&= \overline{A}_\varepsilon \bar{\varepsilon}(t) + \Delta\bar{\varepsilon}(t) + \overline{d}_e(t)
\end{aligned} \tag{19}
$$

where

$$
\overline{A}_\varepsilon = \theta\begin{pmatrix} -2I_4 & I_4 \\ -I_4 & \mathbf{0}_{4\times4} \end{pmatrix}, \Delta\bar{\varepsilon} = \begin{pmatrix} \mathbf{0}_{4\times4} \\ \overline{A}_{22}\varepsilon_2(t)/\theta^2 \end{pmatrix}, \overline{d}_e(t) = \begin{pmatrix} \overline{B}_{d1}/\theta \\ \overline{B}_{d2}/\theta^2 \end{pmatrix} d_e(t).
$$

The eigenvalues of the matrix $\overline{A}_\varepsilon$ is $-\theta$, therefore the error dynamic in (19) can be ensured to be stable. Moreover, the effects from the disturbance terms $\Delta\bar{\varepsilon}(t)$ and $\overline{d}_e(t)$ can be prevailed if a reasonably large θ is chosen.

In terms of (16), the proposed observer can be transformed back into the following form:

$$
\dot{\hat{z}}(t) = F\hat{z}(t) + Gu(t) + O^{-1}L(y(t) - H\hat{z}(t)) \tag{20}
$$

where $\hat{z}(t) = O^{-1}\hat{\xi}(t)$.

Furthermore, from (12) and (20), the observer for the system (10) can be obtained as follows:

$$\dot{\hat{x}}_e(t) = A_e(\lambda, \beta, \omega_r)\hat{x}_e(t) + B_e u(t) + P^{-1}O^{-1}L(y(t) - C_e\hat{x}_e(t)) \quad (21)$$

Where $\hat{x}_e(t) = P^{-1}\hat{z}(t)$.

4.2. Procedure of The Observer Design

The steps of the observer design are as follows:

Step1: Constructing augmented system as Eq.(10);

Step2: Selecting linear transformation matrix *P* and *O*, via twice coordination transformation, generate an observable canonical form of the augmented system;

Step3: Design observer *L* to ensure the error dynamics to be stable.

Step 4: Produce the estimated states $\hat{x} = [I_6 \quad \mathbf{0}_{6\times 2}]\hat{x}_e$, and the reconstructed faults $\hat{f}_{au} = [\mathbf{0}_{1\times 6} \quad 1 \quad 0]\hat{x}_e$ and a $\hat{f}_c = [\mathbf{0}_{1\times 7} \quad 1]\hat{x}_e$.

5. Real-time simulation and validation studies

5.1. Parameter-varying Wind Turbine Modeling

The 4.8MW wind turbine benchmark system is developed under Matlab/Simulink environment, which is utilized to validate the parameter-varying modelling approach addressed in Section 2 of this paper. In this wind turbine benchmark system, the target of power generation is 4.8 MW with a changing wind speed input, shown as Figure 3a. The system measurable outputs are: rotor speed, blade angle, generator torque and generator speed. The responses of the benchmark wind turbine system and the parameter-varying model are shown in Figure 3b-3f, where in order to show clearly, the solid lines, dash-lines and "○" mark have been employed to illustrate the different responses of the benchmark system model and the parameter-varying model in each Figure, respectively. One can see the responses of the parameter-varying model with real-time updating nonlinear polynomial function can well track the responses of the

wind turbine benchmark system under the condition with the same inputs and controller. It is evident that all the parameters of the parameter-vary model are consistent with those of the real-time benchmark system, no matter on the transient responses or steady states.

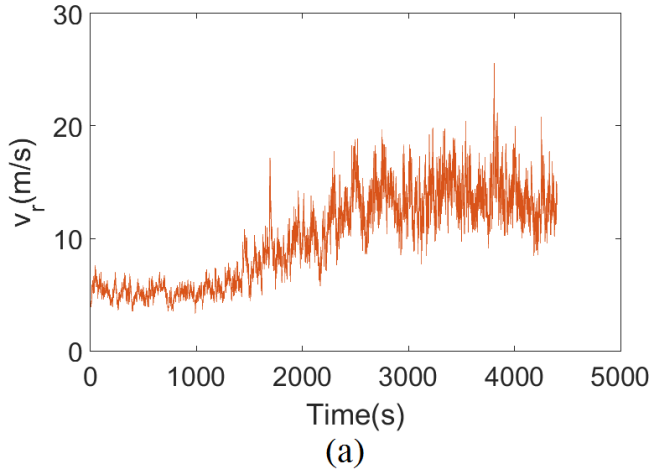

(a)

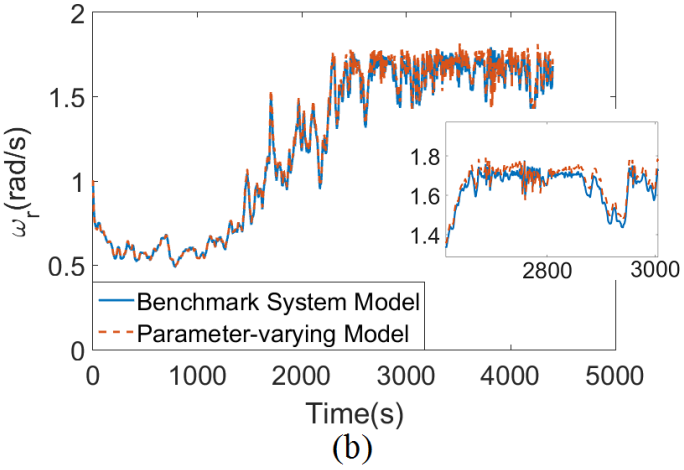

(b)

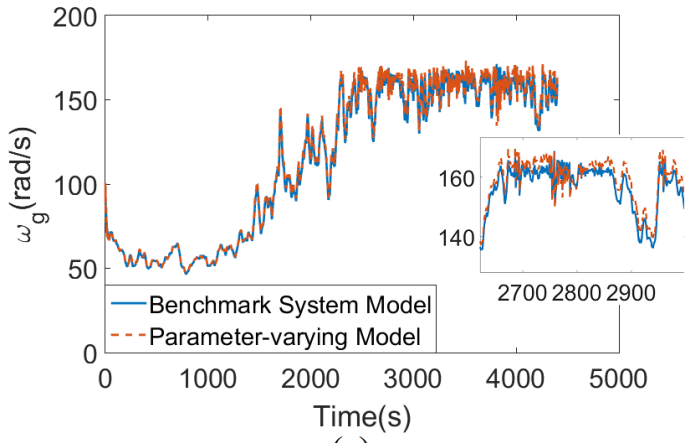

(c)

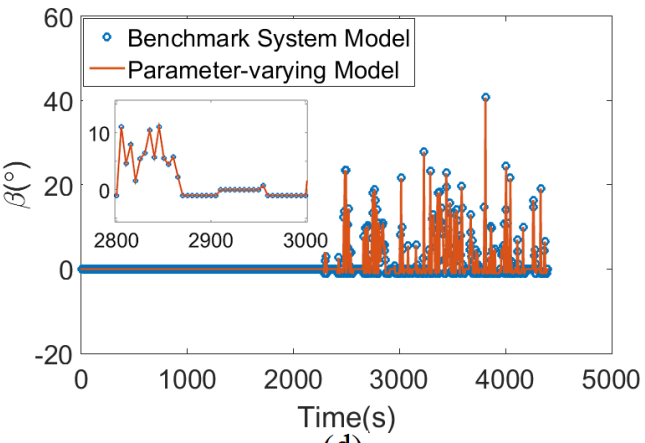

(d)

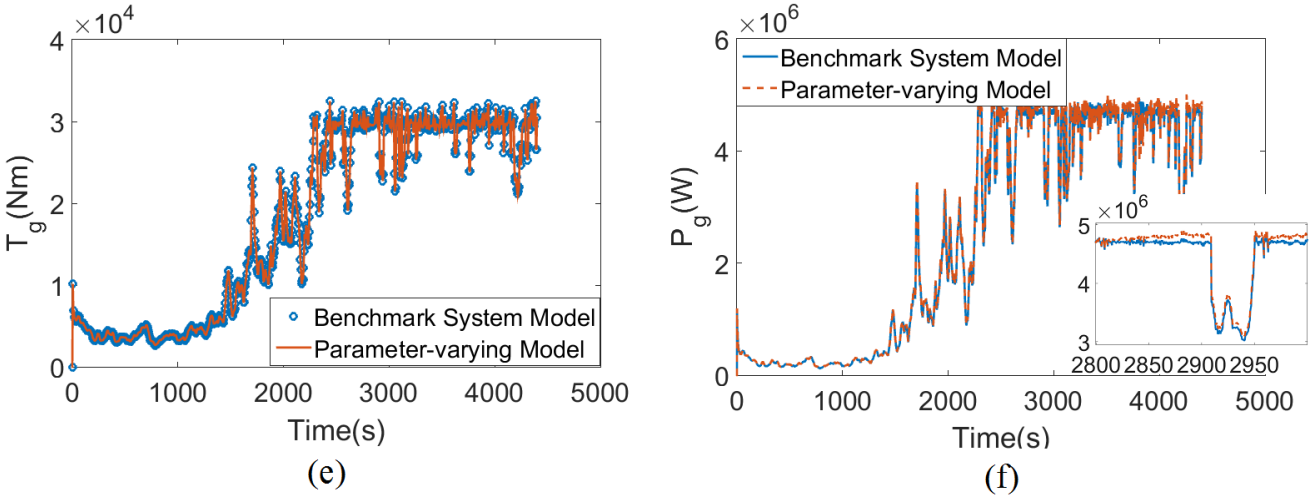

Figure 3. (a) Wind speed;

(b)-(f) States comparison between parameter-varying model and benchmark model.

5.2. Adaptive Parameter-varying Observer for State Estimation and Fault Reconstruction

(i) State estimates

By using adaptive observer with parameter-varying given by (21), one can simultaneously estimate the system states and the concerned faults. Figure 4a-4f show the state variables of the wind turbine system and their estimates, where the solid lines are the estimates and the lines with circle marks denote the system states. One can see that the parameter-varying observer is able to track the states of the benchmark model rapidly. Actually, the state estimates are the by-products of the adaptive observer, from which we can obtain the information of the healthy status of the wind turbine system.

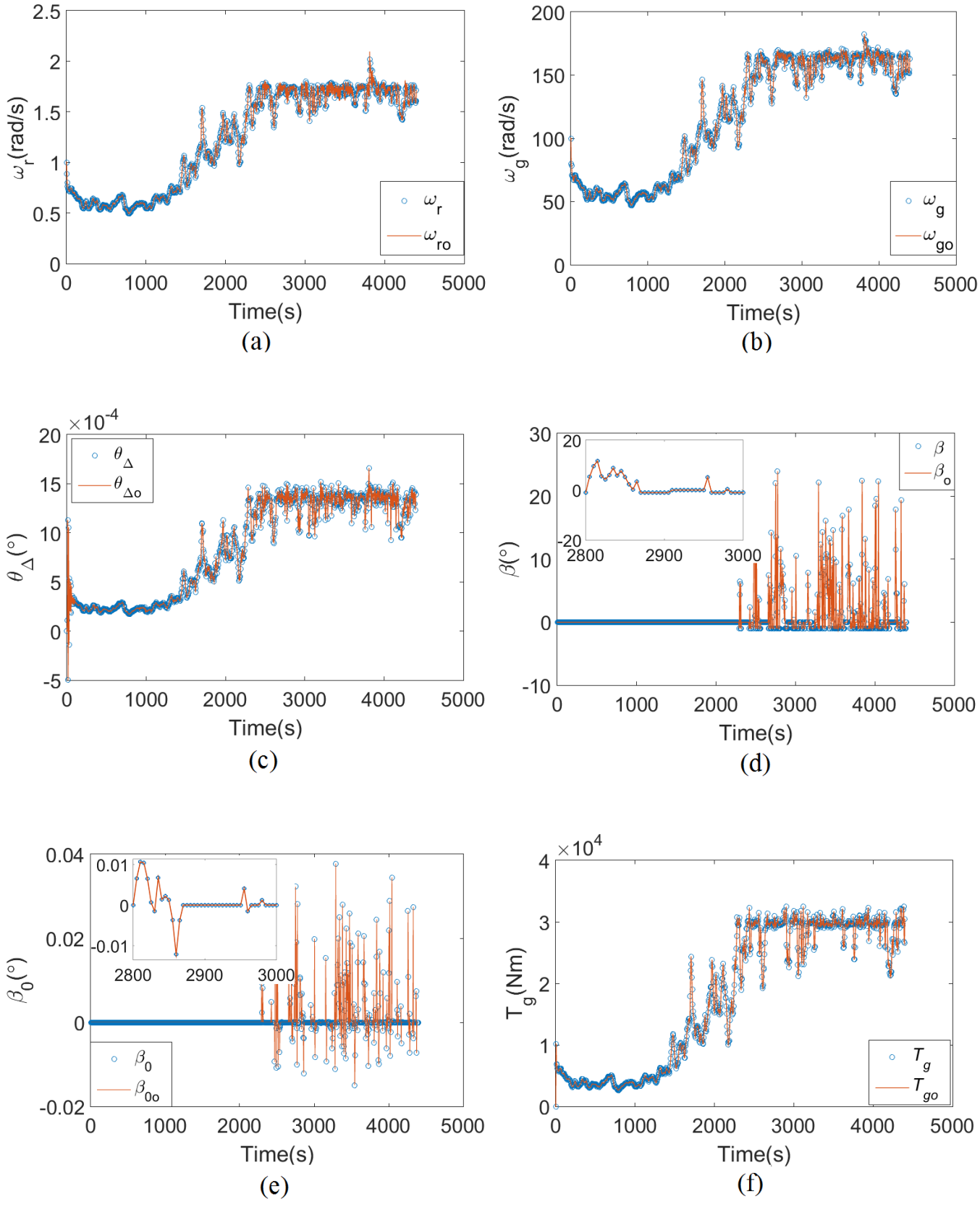

Figure 4. Wind turbine states and their estimates by using the proposed observer

(ii) Fault reconstruction

In the wind turbine system, the actuator fault and component faults are both considered. A band-limit white noise is added as the process disturbance. For the component faults, the viscous friction parameter of the high-speed shaft, described as fault reference value B_{gfr} , has an effect on the term a_{22} in the system matrix, causing the generator speed fault, which is considered as multiplicative term ΔA of the system matrix:

$$B_{gfr}=\begin{cases} 0 & 0\text{s}\le t<1000\text{s} \\ -5\text{Nms/rad} & 1000\text{s}\le t<1500\text{s} \\ 0 & 1500\text{s}\le t<2000\text{s} \\ \dfrac{-5(t-2000)}{500}\text{Nms/rad} & 2000\text{s}\le t<2500\text{s} \\ -5\text{Nms/rad} & t\ge 2500\text{s} \end{cases}$$

For the actuator faults, the generator and converter additive fault would bring a bias for the generator reference torque T_{gfr}:

$$T_{gfr}=\begin{cases} 0 & 0\text{s}\le t<1000\text{s} \\ 200\text{Nms} & 1000\text{s}\le t<1500\text{s} \\ 0 & 1500\text{s}\le t<2000\text{s} \\ \dfrac{200(t-2000)}{500}\text{Nms} & 2000\text{s}\le t<2500\text{s} \\ 200\text{Nms} & t\ge 2500\text{s} \end{cases}$$

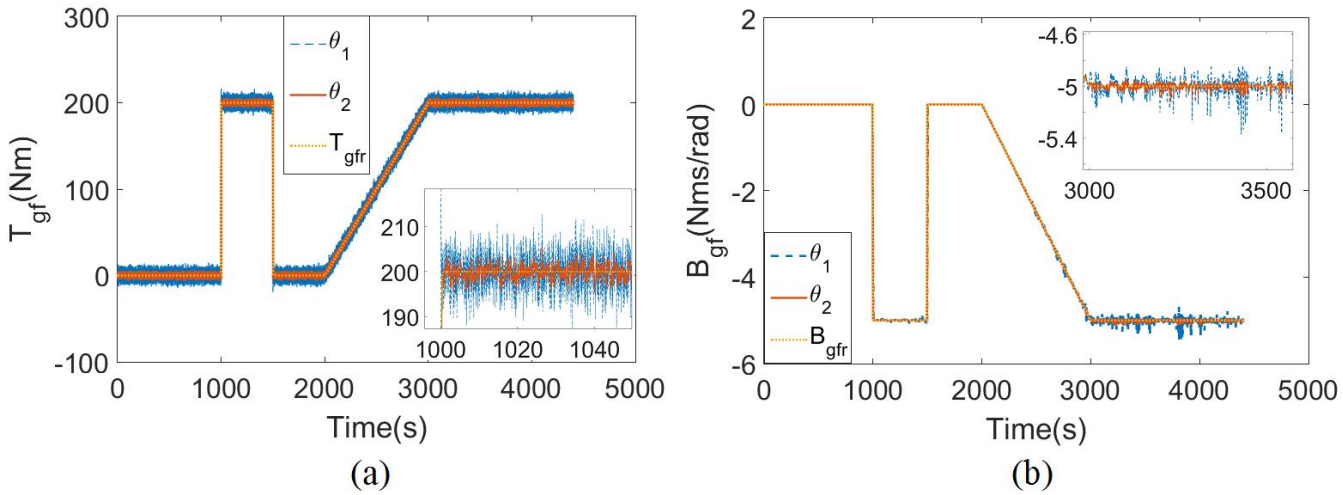

(a) (b)

Figure 5. Faults monitoring; (a) Actuator fault; (b) Component fault

The simulation results for fault reconstructions are shown as Figures 5a and 5b. The reconstructed actuator bias fault and the component fault are obtained, by using the proposed observer with the poles at $\theta_1 = 2$ or $\theta_2 = 10$. One can see the estimated fault signals can well track the actual fault signals with good disturbance attenuation ability. In the meanwhile, the considered faults are intermitted, encouragingly; the proposed fault reconstruction technique can successfully track this kind of challenging faults. As a result, the proposed fault reconstruction technique is effective and powerful.

6. Conclusions

This paper has addressed a novel design for parameter-varying modeling and adaptive observer for fault reconstructions in wind turbine systems. The proposed parameter-varying model is real-time updating nonlinear model, and the proposed fault estimation is adaptive with real-time parameter updating. The fault diagnosis scheme is away from the conventional switching strategy, and the diagnosis process is non-invasive without any effects on the system operation. The effectiveness of the proposed model and fault reconstruction technique has been well demonstrated on the 4.8MW real-time wind turbine system.

In the future, interesting research directions are to use the parameter-varying models to develop fault-tolerant control strategy with real-time parameter regulations, which would significantly improve the reliability and availability of wind turbine energy systems.

References

1. Ribrant, J.; Bertling, L. Survey of failures in wind power systems with focus on Swedish wind power plants during 1997–2005, *IEEE Trans. Energy*. **2007**, 22, 167-173.

2. Gao, Z.; Ding, S.X.; Cecati, C. Real-time fault diagnosis and fault-tolerant control. *IEEE Trans. Ind. Electron.* **2015**, 62, 3752-3756.
3. Gao, Z.; Cecati, C.; Ding, S.X. A survey of fault diagnosis and fault-tolerant techniques—Part I: fault diagnosis with model-based and signal-based approaches, *IEEE Trans. Ind. Electron.* **2015**, 62, 3757-3767.
4. He, X.; Wang, Z.; Liu, Y.; Zhou, D. Least-Squares fault detection and diagnosis for networked sensing systems using a direct state estimation approach , *IEEE Trans. Ind. Inf.* **2013**, 9, 1670-1679.
5. Gao, Z.; Saxen, H.; Gao, C. Data-driven approached for complex industrial systems, *IEEE Trans. Ind. Inf.* **2013**. 9, 2210-2212.
6. Wang, G.; Yin,S.; Kaynak O. An LWPR-based data-driven fault detection approach for nonlinear process monitoring, *IEEE Trans. Ind. Inf.* **2014**, 10, 2016-2023.
7. Wei, X.; Verhaegen, M. Sensor and actuator fault diagnosis for wind turbine systems by using robust observer and filter, *Wind Energy*. **2011**, 14, 491-516.
8. Sun, X.; Patton, R. Robust actuator multiplicative fault estimation with unknown input decoupling for a wind turbine system, *Proc. Conf. Contr. Fault-Tolerant Syst.*, Nice, pp.263-268, Oct., 2013.
9. Zhu, Y.; Gao, Z. Robust observer-based fault detection via evolutionary optimization with applications to wind turbine systems, *Pro. IEEE Conf. Ind. Elec. Appli.*, Hangzhou, pp.1627-1632, Jun. 2014.
10. Odofin, S.; Gao, Z.; Sun, K. Robust fault estimation in wind turbine systems using GA optimization, *Proc. IEEE Conf. Ind. Inf.* **2015**, 580-585, Cambridge.
11. Muljadi, E.; Pierce, P.; Migliore, P. Control strategy for variable-speed, stall-regulated wind turbines, *Proc. American Contr. Conf.*, Philadelphia, PA, Jun. 1998.

12. Hwang I.; Kim S.W.; Kim Y.D.; Seah, C.E. A survey of fault detection, isolation, and reconfiguration methods, *IEEE Trans. on Control Systems Technology*. **2010**, 18, 636-653.
13. Demetriou, M.A. Using unknown input observers for robust adaptive fault detection in vector second-order systems, *Mechan. Syst. Signal Process*. **2005**, 19, 291–309.
14. Saheb-Koussa, D.; Haddadi, M.; Belhamel, M.; Said, M. Modeling and simulation of wind generator with fixed speed wind turbine under Matlab-Simulink, *Energy Procedia*. **2012**, 18, 701-708.
15. Tabatabaeipour, S.M.; Odgaard, P.F.; Bak, T.; Stoustrup, J. Fault detection of wind turbines with uncertain parameters: A Set-Membership Approach, *Energies*. **2012**, 5, 2424-2448.
16. Cao, G.; Grigoriadis, K.; Nyanteh, Y. LPV control for the full region operation of a wind turbine integrated with synchronous generator, *Scientific World Journal.* **2015**, 1-15.
17. Bianchi, F.; Mantz, R.; Christiansen, C. Control of variable-speed wind turbines by LPV Gain Scheduling, *Wind Energy*. **2004**, 7, 1-8.
18. Jiang, B.; Zhang, K.; Shi, P. Integrated fault estimation and accommodation design for discrete-time Takagi–Sugeno fuzzy systems with actuator faults, *IEEE Trans. On Fuzzy Systems*. **2011**, 19, 291-304.
19. Liu, X.; Gao, Z; Chen M. Takagi-Sugeno fuzzy model based fault estimation and signal compensation with application to wind turbines, *IEEE Trans. On Industrial Electronics*, Mar. 2017.
20. Xu, Z.; Hu, Q.; Ehsani, M. Estimation of effective wind speed for fixed-speed wind turbines based on frequency domain data fusion, *IEEE Trans. On Sustainable Energy*. **2012**, 3, 57-64.
21. Díaz de Corcuera, A.; Pujana-Arrese, A.; Ezquerra, J.; Landaluze, A. Linear models-based LPV modelling and control for wind turbines, *Wind Energy*. **2015**, 18, 1151-1168.
22. Simani, S.; Castaldi, P. Adaptive fault–tolerant control design approach for a wind turbine benchmark, *Proc. 8th IFAC Symp. Fault Detection, Supervis., Safety Tech. Processes*. (Safeprocess), Mexico City, Mexico, pp. 319–324, Aug. 2012.

340 23. Tohidi, A.; Hajieghrary, H.; Hsieh, M.A. Adaptive disturbance rejection control scheme for DFIG-
341 based wind turbine: theory and experiments, *IEEE Trans. On Industry Applications*. **2016**, 52, 2006-
342 1015.
343 24. Chen, J.; Jiang, L.; Yao, W.; Wu, Q.H. Perturbation estimation based nonlinear adaptive control of a
344 full-rated converter wind turbine for fault ride-through capability enhancement, *IEEE Trans. On*
345 *Power Systems*. **2014**, 29, 2733-2743.
346 25. Odgaard, P.; Stoustrup, J.; Kinnaert, M. Fault-tolerant control of wind turbines: A benchmark model,
347 *IEEE Trans. on Control Systems Technology*. **2013**, 21, 1168-1182.
348 26. Song, Y.D.; Zhao, K.; Krstic, M.A. Control with exponential regulation in the absence of persistent
349 excitation, *IEEE Trans. on Automatic Control*, **2016**. (DOI 10.1109/TAC.2016.2599645)
350 27. Solo, V. Time varying parameters in adaptive control: a review and a preview, *Proc. of 31th Conf. on*
351 *Decision and Control*, pp.684-687, 1992.
352 28. Xu, J.X. A New Periodic adaptive control approach for time-varying parameters with known
353 periodicity, *IEEE Trans. On Automatic Control*. **2004**, 49, 579-583.
354 29. Jonson, Kathryn E.; Pao, Lucy Y.; Balas, Mark J. and Fingersh, Lee J. Control of variable-speed
355 wind turbines: standard and adaptive techniques for maximizing energy capture, *IEEE Control*
356 *Systems Magazine*. **2006**, 26(3):70-81.

357 **Acknowledgement**

358 The work is supported by the China Scholarship Council (CSC201407540009), the E&E faculty at the
359 University of Northumbria.
360